

Computational Investigation of the Solvation of Nitric Acid: Formation of the NO_3^- and H_3O^+ Ion Pair

Jill R. Scott^{*,†} and J. B. Wright[‡]

Idaho National Engineering and Environmental Laboratory, 2525 North Fremont Avenue, Idaho Falls, Idaho 83415, and Natick Soldier Center, U.S. Army RDECOM, AMSRD-NSC-SS-MS, Natick, Massachusetts 01760

Received: June 1, 2004; In Final Form: July 30, 2004

MP2 and B3LYP calculations were performed on complexes of nitric acid with water using the 6-311++G(2d,p) basis set to determine optimized geometries and binding energies for $\text{HNO}_3 \cdots n\text{H}_2\text{O}$ systems ($n = 1-4$). The structures for the global minima for $n = 1-4$ have homodromic rings formed by successive hydrogen bonds. The potential energy surface for the $\text{HNO}_3 \cdots n\text{H}_2\text{O}$ clusters is quite shallow. The first stable ion-pair configuration is obtained for a $\text{HNO}_3 \cdots 4\text{H}_2\text{O}$ complex. The ion pair, $\text{H}_3\text{O}^+ - \text{NO}_3^-$, is separated by the three H_2O molecules forming an Eigen-ion (H_9O_4^+) type structure. The transition states and activation barriers for $n = 1-4$ were also determined. The zero-point corrected transition-state barrier for the ion pair is only 0.5 kcal/mol. Larger $\text{HNO}_3 \cdots n\text{H}_2\text{O}$ clusters (n up to 32) were also determined to be dominated by the ion-pair motif.

Introduction

Nitric acid is important to diverse areas such as atmospheric chemistry^{1,2} and nuclear waste.³⁻⁶ Computational studies of nitric acid and nitrate have primarily focused on their importance in the atmosphere. Our focus is on nitrate within nuclear wastes. While most nuclear wastes are basic, some of the nuclear waste stored at the Idaho National Engineering and Environmental Laboratory (INEEL) is acidic.⁷ The amount of water in the waste varies significantly to the point that there may not be sufficient water molecules to fully solvate the alphabet soup of ions present (e.g., Al^{3+} , Be^{2+} , Cd^{2+} , Dy^{3+} , Eu^{3+} , etc.). Of the few anions present, nitrate is by far the dominant anion in the acidic waste. Our interest is in computationally determining how many waters are necessary to form the NO_3^- and H_3O^+ ion pair and how that ion pair behaves in a solvated system. Experimental evidence suggests that ionization of nitric acid may require as few as two or as many as 10 water molecules.⁸⁻¹⁰

The focus of computations for nitric acid and water clusters has been related to their importance as isolated complexes in atmospheric chemistry. The most computationally studied structure for nitric acid and water interaction is the nitric acid monohydrate (NAM) complex. In 1991, Koller and Hadži¹¹ reported geometries for both the neutral ($\text{HNO}_3 \cdots \text{H}_2\text{O}$) and ionized ($\text{NO}_3^- \cdots \text{H}_3\text{O}^+$) structures for the NAM using semi-empirical and ab initio methods. The neutral complex was found to be energetically more favorable, which agreed well with experimental evidence of neutral NAM in glass.^{12,13} The structure of the neutral $\text{HNO}_3 \cdots \text{H}_2\text{O}$ complex was found to be almost planar with a six-membered ring formed by two oxygens, the nitrogen, and the hydrogen of the nitric acid and the oxygen and one hydrogen of the water. One distinctly linear hydrogen bond between the water and the nitric acid was discernible with a second very bent hydrogen–oxygen interaction. Koller and

Hadži¹¹ also reported structures for ionic versions of the nitric acid pair, H_3O^+ and NO_3^- , by artificially constraining the calculations. Interaction energies were calculated for the various basis sets used and found to range from -7.49 to -19.01 kcal/mol. Higher level calculations, MP2/6-311++G(2d,p), were performed by Tao et al.¹⁴ to deduce the structure of NAM, which is very similar to that observed by Koller and Hadži.¹¹ Tao et al.¹⁴ found that the strongest hydrogen bond is formed between the hydrogen of the nitric acid and the oxygen of the water with a bond length of 1.71 Å and is only slightly bent ($\sim 176^\circ$). A second hydrogen bond is formed between a hydrogen on the water and an oxygen on the nitric acid that is considerably weaker than the first hydrogen bond. The structure by Tao et al.¹⁴ was confirmed by Canagaratna et al.¹ with microwave spectroscopy. Canagaratna et al.¹ and others^{11,14} have remarked that this second hydrogen bond barely meets the definition of a H bond because it is extra long (2.3 Å) and extremely bent ($\sim 120^\circ$); however, it does provide extra stability for the complex. The dissociation energy without zero-point correction (D_e) was calculated to be -9.5 kcal/mol, and with zero-point correction (D_0) it was calculated to be -7.2 kcal/mol.¹⁴ Tóth¹⁵ also focused on NAM both in the gas phase and in the bulk crystalline structure. Several basis sets were employed for the gas-phase calculations with all of the ab initio calculations giving essentially the same geometry as reported by Tao et al.¹⁴ The binding energies for the density functional theory (DFT) calculations were on the same order as that previously reported.¹⁴ Staikova and Donaldson¹⁶ also investigated the geometry and energetics of NAM using Moller–Plesset theory (MP2) and DFT computations using the extensive 6-311++G(3df,3dp) basis set, with similar results.

In addition to NAM, McCurdy et al.¹⁷ and Escibano et al.¹⁸ studied larger $\text{HNO}_3 \cdots n\text{H}_2\text{O}$ complexes in the gas phase. McCurdy et al.¹⁷ looked at nitric acid interaction with up to four water molecules using the MP2 level of theory with the aug-cc-pVDZ basis set. For nitric acid dihydrate (NAD) and nitric acid trihydrate (NAT) systems, the $\text{HNO}_3 \cdots n\text{H}_2\text{O}$ ($n =$

[†] Idaho National Engineering and Environmental Laboratory.

[‡] Natick Soldier Center/U.S. Army RDECOM.

TABLE 1: Binding Energies and TS Barriers for $\text{HNO}_3 \cdots n\text{H}_2\text{O}$ ($n = 1-4$)^a

cluster	D_e^{uncor}	D_e^{ZPC}	D_0	$\Delta E_{\text{uncor}}^\ddagger$	$\Delta E_{\text{ZPC}}^\ddagger$
$\text{HNO}_3 \cdots 1\text{H}_2\text{O}$	-10.2 (-10.6)	-10.2 (-8.5)	-9.3 (-6.5)	13.3	11.1
$\text{HNO}_3 \cdots 2\text{H}_2\text{O}$	-20.5 (-21.6)	-18.2 (-17.0)	-16.4 (-12.9)	11.5	9.1
$\text{HNO}_3 \cdots 3\text{H}_2\text{O}$	-29.7 (-31.6)	-25.2 (-24.6)	-22.4 (-18.3)	11.9	9.9
$\text{HNO}_3 \cdots 3\text{H}_2\text{O}$ (alternative)	-29.6 (-32.0)	-25.0 (-25.0)	-22.4 (-18.6)	11.1	9.3
$\text{HNO}_3 \cdots 4\text{H}_2\text{O}$ (cyclic)	-39.2 (-42.4)	-32.4 (-33.1)	-23.5 (-24.1)	9.3	7.2
$\text{HNO}_3 \cdots 4\text{H}_2\text{O}$ (alternative cyclic)	-39.7 (-42.7)	-32.8 (-33.4)	-24.3 (-24.9)	8.2	7.0
$\text{HNO}_3 \cdots 4\text{H}_2\text{O}$ (ion pair)	-36.8 (-41.0)	-28.9 (-30.6)	-24.3 (-16.3)	2.8	0.5

^a B3LYP/6-311++G(2d,p) listed first with MP2/6-311++G(2d,p) values given in parentheses. Energy units are kcal/mol.

2, 3) structures consisted of homodromic rings with the nitric acid and each water forming two hydrogen bonds. These cyclic geometries had binding energies of 20.6 (16.2) kcal/mol and 30.4 (23.7) kcal/mol, respectively (values in parentheses correspond to zero-point corrected (ZPE) binding energies). Escribano et al.¹⁸ used the B3LYP level of theory with the aug-cc-pVTZ basis set for NAD and NAT geometries and obtain similar cyclic structures and slightly lower binding energies (~ 2 kcal/mol lower) than those reported by McCurdy et al.¹⁷ for the same geometries. Koller and Hadži¹¹ also optimized structures for NAT, but did not find cyclical structures with the methods employed. McCurdy et al.¹⁷ also reported two structures for the $\text{HNO}_3 \cdots 4\text{H}_2\text{O}$ complex. One structure continues the homodromic ring motif and was reported to be the global minimum within the structures explored. The other geometry showed the formation of the nitrate/hydronium ion pair but was only considered a local minimum because its energy was found to be 0.4 kcal/mol higher than the neutral, cyclic structure. The binding energies for the cyclic and ion-pair geometries were reported as 40.5 (31.4) kcal/mol and 40.1 (29.9) kcal/mol, respectively.

In this paper, we explore the formation of nitric acid/water clusters ($\text{HNO}_3 \cdots n\text{H}_2\text{O}$). The ground-state (GS) geometries and binding energies are compared to previous works for clusters with $n = 1-4$. The transition states (TS's) and activation energies were calculated to reveal insights into the solvation mechanisms, focusing on the nature of the solvated proton. Results for $\text{HNO}_3 \cdots n\text{H}_2\text{O}$ complexes with $n > 7$ are also discussed.

Computational Methods

Ab initio and DFT molecular orbital calculations for $\text{HNO}_3 \cdots n\text{H}_2\text{O}$ systems ($n = 1-4$) were performed using the Gaussian 98¹⁹ and Gaussian 03²⁰ series of programs. Initial calculations explored different geometries for HNO_3 and $n\text{H}_2\text{O}$, as well as starting with the ions NO_3^- and H_3O^+ with $n\text{H}_2\text{O}$, using the B3LYP exchange and correlation functionals^{21,22} with the 6-31G(d,p) basis set.²³⁻²⁸ For the $\text{HNO}_3 \cdots n\text{H}_2\text{O}$ systems where $n = 1-4$, the lowest energy structures were fully optimized at the B3LYP/6-311++G(2d,p) level of theory to account for diffuse functions on both the heavy atoms and hydrogens. To include correlation contributions, single-point MP2 (spMP2) energies were calculated for the B3LYP/6-311++G(2d,p) geometries. Second-order Moller–Plesset perturbation theory (MP2)^{29,30} with the 6-311++G(2d,p) basis set calculations were also performed to obtain fully optimized geometries and energies. A comparison of the geometries determined that B3LYP/6-311++G(2d,p) results were very similar to those using MP2/6-311++G(2d,p). The spMP2 energies for the B3LYP structures were also very close to the energies obtained with fully optimized geometries and energies at the MP2 level of theory. All minimizations were carried out using the Bery algorithm^{31,32} using the default Gaussian

parameters for the integral cutoff and minimization convergence criteria. Vibrational frequencies were calculated for all minima at all levels of theory to obtain zero-point energies and to ensure that the TS's had only one imaginary frequency while all minima had zero imaginary frequencies.

It is generally accepted that binding energies need to be corrected for the basis set superposition error (BSSE) for comparison with experimental values.³³⁻³⁶ The counterpoise method^{37,38} was employed, because it is the generally accepted methodology to compensate for BSSE.³⁹⁻⁴¹ Application of the BSSE correction has been known to change the order of local minima from that predicted by the uncorrected energies.⁴² The BSSE correction is especially necessary for weakly bound complexes; however, the nitric acid and water complexes have been found to be strongly bound with BSSE corrections being essentially negligible (2–3%) using B3LYP/6-311++G-(3df,2dp);¹⁶ therefore, the BSSE corrections were not included in several of the previous literature reports for $\text{HNO}_3 \cdots n\text{H}_2\text{O}$ systems.^{39,40,43} The BSSE correction factors are reported in the tables in Supporting Information. For convenience in comparison with previous literature values, uncorrected, ZPC, and ZPC + BSSE corrected binding energies are reported in Table 1. It should be noted that the BSSE does vary depending on the level of theory with the values for the MP2/6-311++G(2d,p) being approximately a factor of 2 or 3 greater than those for the DFT calculations using the same basis set as seen in Tables 2S–8S in Supporting Information.

Comprehensive lists of structural and energy parameters for the $n = 1-4$ systems, as well as the monomers, are given in Supporting Information. The convention used in this paper is to label the water hydrogens that participate in hydrogen bonds with an “a” as in H_{1a} , while those that do not participate are designated with a subscript “b”.

Results and Discussion

Systems with multiple hydrogen bonds have been explored by other research groups to investigate the effect of correlation energy and basis set on the geometries and energies.⁴⁴ As noted in the introduction, small clusters of nitric acid with water have been studied using a variety of computational methods including MP2/6-311++G(2d,p),¹⁴ MP2/aug-cc-pVDZ,¹⁷ B3LYP/aug-cc-pVTZ,¹⁸ and B3LYP/6-311++G(3df,2dp).¹⁶ While there are some minor variations among the results for the different methods for the GS structures, the overall agreement between the more comprehensive basis sets is reassuring. Because there are no literature references for the TS structures, the quality of these calculations can only be assessed in light of the consistency of the GS structures.

In general, the structures for the isolated $\text{HNO}_3 \cdots n\text{H}_2\text{O}$ systems ($n = 1-4$) is the formation of planar ring structures. Following Tzeli et al.,⁴² McCurdy et al.¹⁷ applied the term “homodromic” to describe the network of successive H bonds in the same direction around a quasi-planar ring. In the TS's,

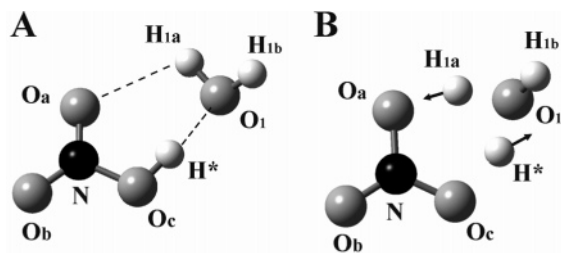


Figure 1. Structures of the $\text{HNO}_3 \cdots \text{H}_2\text{O}$ cluster for the (A) GS and (B) TS with solid arrows indicating displacement vectors. Color scheme is nitrogen = black, oxygen = gray, and hydrogen = white.

the transfer of hydrogens around the homodromic rings is reminiscent of early descriptions of proton conduction as a successive proton-transfer chain mechanism⁴⁵ named after de Grötthuss⁴⁶ for his work on electrolysis of salt solutions.⁴⁷ Of course, the mechanism of proton mobility has been and still is debated.^{45,48–53} Systems where $n \geq 4$ show the formation of the ion pair and are of the most interest for solvated nitric acid. In these more solvated complexes, the nitrate exists in its C_{3v} monomeric state and the proton appears as an Eigen-ion (H_9O_4^+)⁵³ type structure.

$\text{HNO}_3 + \text{H}_2\text{O}$ System. Several starting geometries were considered, but the structure in Figure 1A was determined to be the global minimum of those studied. Structures for the alternative local minimum have been reported by Staikova et al.¹⁶ for computations using B3LYP level of theory with the more extensive 6-311++G(3df,3dp) basis set than that used in the current calculations. These structures show the hydrogens of the water molecule interacting with the unprotonated oxygens of the nitric acid in various configurations. Escribano et al.¹⁸ and McCurdy et al.¹⁷ also reported finding at least one energetically less favorable structure. The potential energy barriers between these structures are very small (<2 kcal/mol). Initial geometries using the ions NO_3^- and H_3O^+ merely relaxed into an optimized geometry for a neutral complex. This result for the isolated complex is not surprising because experimental results for HNO_3 and H_2O in glass indicate that the neutral complex dominates.^{12,13} Additional experimental evidence for the neutral $\text{HNO}_3 \cdots \text{H}_2\text{O}$ complex comes from hydration studies of nitric acid in benzene.¹⁰

The GS structure for the $\text{HNO}_3 \cdots \text{H}_2\text{O}$ complex (Figure 1A) is the same as that calculated by Tao et al.¹⁴ and reported by other researchers.^{16–18} The structure is a six-membered ring formed using two hydrogen bonds between the nitric acid and the water molecule that is essentially planar with one of the water hydrogens (H_{1b}) projecting out of the plane (Figure 1A). Detailed parameters are provided in Table 2S in Supporting Information. Regardless of the level of theory and basis set used, most ab initio and DFT calculations produce a similar structure.^{14–18} While the structures obtained for the monohydrate complex are similar, there are differences in the binding energy depending on the computational method. The calculated binding energies range from -19.0 kcal/mol to -7.0 kcal/mol.^{14–18} Overall, the uncorrected binding energy (D_e) is close to -10 kcal/mol, such as -10.3 kcal/mol obtained using MP2/aug-cc-pVDZ by McCurdy et al.,¹⁷ which agrees well with the uncorrected value of -10.2 kcal/mol from the B3LYP/6-311++G(2d,p) calculation. Using a larger basis set with B3LYP, Staikova and Donaldson¹⁶ reported a D_e value of -9.6 kcal/mol. The overall corrected binding energy is approximately -7 kcal/mol, but the reported values do depend on the correction factors applied. For example, Tao et al.¹⁴ used a ZPE energy of 2.3 kcal/mol derived using the 6-31+G(d) basis set, instead of

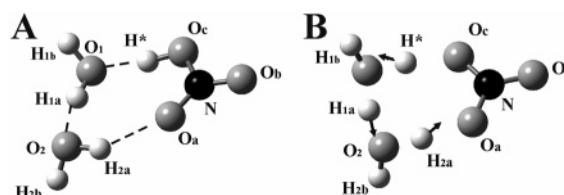


Figure 2. Structures of the $\text{HNO}_3 \cdots 2\text{H}_2\text{O}$ cluster for the (A) GS and (B) TS with solid arrows indicating displacement vectors. Color scheme is nitrogen = black, oxygen = gray, and hydrogen = white.

6-311++G(2d,p), to correct the binding energy to a value of $D_0 = -7.5$ kcal/mol. The MP2/6-311++G(2d,p) fully corrected binding energy calculated in this work is -6.5 kcal/mol (Table 1). A discussion of the various correction procedures employed and how they apply to “true” binding energies is beyond the scope of this paper. The values listed in Table 1 and in Tables 1S–9S are provided primarily for comparison between structures.

The TS structure for the $\text{HNO}_3 \cdots \text{H}_2\text{O}$ cluster was also determined and is provided in Figure 1B. Detailed parameters are provided in Table 2S. The TS geometry is still nearly planar with a dihedral of -179.7° . The primary difference between the TS and the GS structure is in the symmetry of the two hydrogen bonds, which both have lengths of 1.114 Å and an O–H–O angle of 153.1° in the TS. The H-bond protons (H^* , H_{1a}) and the water $\text{O}_1\text{–H}_{1b}$ group form a distorted hydronium ion (H_3O^+) motif. The angle $\text{H}_{1a}\text{–O–H}^*$ is only 84.5° in the TS while the H–O–H angles for the hydronium monomer (Figure 1C, Table 1S) are 111.9° . In the TS, the hydrogens involved in the H bonds are simultaneously shuffled around the six-membered ring as illustrated by the displacement vectors (Figure 1B). This hydrogen migration requires that four bonds be simultaneously made/broken. The activation barrier for the TS (ΔE^\ddagger) is 13.3 or 11.1 kcal/mol with zero-point correction.

The NAM can be compared with the monohydrates of other oxyacids, such as triflic⁵⁴ and sulfuric acid.⁵⁵ Paddison et al.⁵⁴ reported the molecular modeling of triflic or trifluoromethanesulfonic acid ($\text{CF}_3\text{SO}_3\text{H}$) interaction with one water molecule. This system also formed a six-membered ring involving the sulfur and two oxygens of the sulfonate, triflic acid proton, and OH of the water molecule. The hydrated triflic acid structure is also stabilized by two H bonds, one long and one short, similar to the structure for $\text{HNO}_3 \cdots \text{H}_2\text{O}$ (Figure 1A). The TS for the proton transfer in triflic acid was found to have an activation barrier of 4.7 kcal/mol, which is less than that for nitric acid as expected. Arstila et al.⁵⁵ did not find a cyclic structure for the monohydrate of sulfuric acid. Instead, only one H bond was formed between the H_2SO_4 and the H_2O with the lowest energy configuration involving the proton donation from the sulfuric acid to the water oxygen. The binding energy was found to be -38 kJ/mol (4.3 kcal/mol), which is twice that of the water dimer (-18 kJ/mol or 8.6 kcal/mol).⁵⁵ As with nitric acid, one water molecule cannot ionize either triflic or sulfuric acid.

$\text{HNO}_3 + 2\text{H}_2\text{O}$ System. Addition of a second water molecule to form the $\text{HNO}_3 \cdots 2\text{H}_2\text{O}$ complex results in a cyclical structure as shown in Figure 2A. A similar structure was also found by McCurdy et al.¹⁷ and Escribano et al.¹⁸ The GS structure is again a homodromic ring with the first H bond in the complex formed between the H^* of nitric acid and the oxygen of the first water (O_1). The detailed parameters using B3LYP and MP2 for the dihydrate complex are provided in Table 3S in Supporting Information. The binding energy for the dihydrate global minimum is approximately twice that of the monohydrate (Table 1).

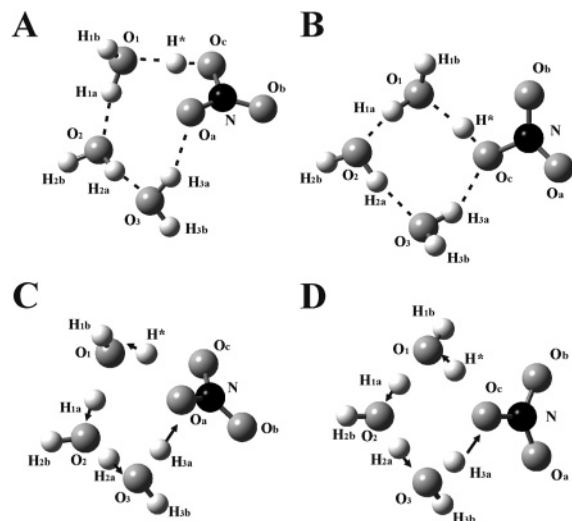


Figure 3. Structures for the $\text{HNO}_3 \cdots 3\text{H}_2\text{O}$ clusters for the (A) GS and (C) TS for cyclic structure 3A. The (B) GS and (D) TS are the structures for a geometry referred to as alternative cyclic structure 3B. Solid arrows indicate displacement vectors for TS's. Color scheme is nitrogen = black, oxygen = gray, and hydrogen = white.

Figure 2B shows the TS structure for the $\text{HNO}_3 \cdots 2\text{H}_2\text{O}$ cluster with detailed parameters provided in Table 3S. The TS geometry is essentially symmetrical and planar similar to the monohydrate TS. Only H_{1b} and H_{2b} are out of the plane, pointing above and below, respectively. The $r(\text{O}_1\text{O}_2)$ in the GS geometry is 2.7 Å, which is longer than the 2.5 Å estimated for the Zundel ion⁵⁶ (H_5O_2^+).^{57,58} However, in the TS state, this interoxygen distance is 2.4 Å and the proton is shared equally between O_1 and O_2 . In the dihydrate TS, as in the monohydrate TS, the hydrogens involved in the H bonds migrate concurrently around the eight-membered ring as illustrated by the displacement vectors (Figure 1B). This proton-relay-type mechanism⁴⁵ involves six bonds being concomitantly made/broken. The activation barrier for the TS (ΔE^\ddagger) is estimated as 11.5 or 9.1 kcal/mol with zero-point correction.

$\text{HNO}_3 + 3\text{H}_2\text{O}$ System. Early 1991 calculations by Koller and Hadži¹¹ did not find a cyclical structure for the $\text{HNO}_3 \cdots 3\text{H}_2\text{O}$ complex; however, these calculations were limited in scope because of the computing power at the time. More recent calculations by McCurdy et al.¹⁷ and Escribano et al.¹⁸ did find cyclical geometries similar to that in Figure 3A. This 10-member ring geometry is referred to as cyclic structure 3A, and its parameters are given in Table 4S in Supporting Information. The TS structure is given in Figure 3C with parameters in Table 4S. For this trihydrate configuration, the TS geometry is very similar to that of the GS with the protons more evenly spaced between consecutive oxygens resulting in a unique TS with electron flow through the 10-membered ring with eight bonds being made/broken simultaneously correlating to one imaginary frequency, as shown by the displacement vectors (Figure 3C). The uncorrected activation barrier for this complex is 11.9 kcal/mol (Table 1).

An alternative structure for hydration of nitric acid with three H_2O molecules where the cyclic ring only includes the one oxygen of the nitric acid, forming an eight-member ring, was also found (Figure 3B). This structure is similar to one reported by Escribano et al.¹⁸ and is referred to as alternative cyclic structure 3B, parameters for which are given in Table 5S. The trend in the hydrogen bond strengths is the same as that for cyclic structure 3A with the $\text{H}^* \cdots \text{O}_1$ bond being the strongest with the others becoming progressively weaker around the

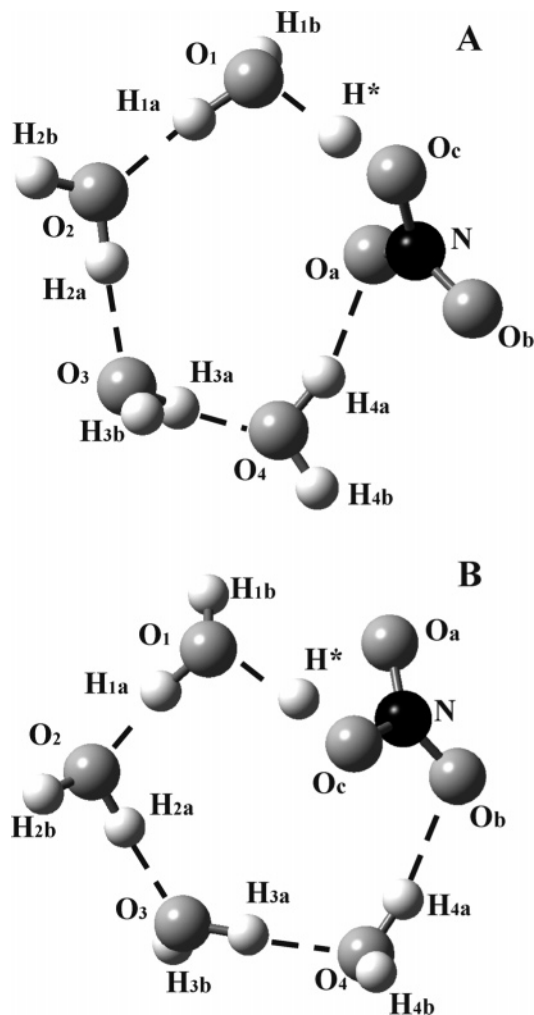


Figure 4. GS structures for two different cyclic geometries for the $\text{HNO}_3 \cdots 4\text{H}_2\text{O}$ cluster referred to as (A) cyclic structure 4A and (B) alternative cyclic structure 4B. Color scheme is nitrogen = black, oxygen = gray, and hydrogen = white.

H-bond circle. However, $\text{H}_{1a} \cdots \text{O}_2$ and $\text{H}_{2a} \cdots \text{O}_3$ are very similar. The TS geometry for the alternative cyclic structure 3B is given in Figure 3D with parameters in Table 5S. As the hydrogens simultaneously shuffle around the eight-membered ring, the N— O_c bond rocks from side-to-side. This TS also involves the eight bonds that are concurrently made/broken and has an uncorrected activation barrier of 11.1 kcal/mol (Table 1).

Escribano et al.¹⁸ assigned structure 3A as the global minimum being 3.2 kJ/mol (0.8 kcal/mol) below structure 3B. Using the basis set 6-311++G(2d,P), assignment of the global minimum depends on the level of theory employed. For B3LYP, structure 3A is more stable than 3B by a mere 0.1 kcal/mol. The order is reversed for the MP2 calculations with 3B more stable by 0.4 kcal/mol. The binding energies for the two structures are also virtually equivalent for B3LYP and only slightly different for MP2 (Table 1). TS barriers determined at the B3LYP level predict that structure 3B has a lower activation energy by ~ 0.6 kcal/mol. Regardless of which structure is assigned as the global minimum, neither structure shows the ability of three waters to ionize nitric acid as has been predicted by experiments.⁹

$\text{HNO}_3 + 4\text{H}_2\text{O}$ Systems. Structures for three distinct minima were obtained for the $\text{HNO}_3 \cdots 4\text{H}_2\text{O}$ complex shown in Figures 4 and 5. Two different versions of cyclic geometries with homodromic rings of water are shown in Figure 4. Figure 5

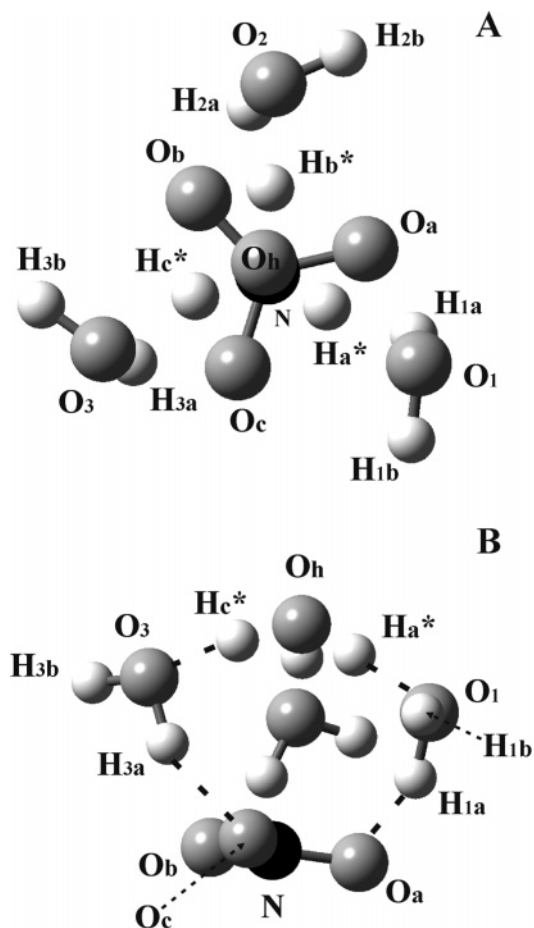


Figure 5. GS structure for HNO₃...4H₂O cluster geometry of the NO₃⁻ and H₃O⁺ ion pair. (A) Side view of the geometry with labels for the second H₂O in the background left out for clarity. (B) Top-down view of the H₃O⁺ over the NO₃⁻. Color scheme is nitrogen = black, oxygen = gray, and hydrogen = white.

shows two views of the GS geometry for the H₃O⁺–NO₃⁻ pair with three waters. The parameter tables for these three structures are available in Tables 6S–8S in Supporting Information, respectively. The ion-pair geometry (Figure 5) and cyclic structure (Figure 4A) have been reported previously by McCurdy et al.¹⁷ however, no structural parameters were reported. As with smaller nitric acid and water systems,^{16,17} the potential energy surface for the four-water complex is quite shallow, with all three structures within less than 1.8 kcal/mol of each other based on MP2 calculated energies. While we only found minima for these three structures after trying a host of combinations starting with nitric acid and water as well as nitrate, hydronium ion, and water, it is possible that other minima may exist.

Two different cyclic structures were found and are given in Figure 4A,B with their detailed parameters given in Tables 6S and 7S, respectively. These structures carry on the homodromic motif characteristic of the smaller HNO₃...*n*H₂O (*n* = 1–3) clusters. As in the two- and three-water systems, the H bonds get longer and the O–O distances increase as one moves from the H* around the ring. The waters further away from H* also begin to look more like the monomer structure. The primary difference between these two structures is that the homodromic ring of cyclic structure 4A makes connections on the nitric acid between the hydrogen (H*) and O_a, which the H* is bent toward. In the alternative cyclic structure 4B, H* is bent away from the nitrate oxygen (O_b) that is used to complete the H-bond cycle. Using the B3LYP calculations, the dihedral angle of the nitric

acid for the alternative cyclic structure 4B is –164°, which indicates that it is not as flat as structure 4A with a dihedral of –172°. However, the MP2 calculations have the dihedral of both structures as –168°. Comparing the parameters in Tables 6S and 7S reveals that the distances for the two structures are quite similar. There are more discrepancies among the angles. For example, ∠O_aNO_c is 3° less for the alternative structure 4B. The trend for the H bonds is about the same for both structures except for the last one in the ring. The bond length H_{4a}...O_a is either slightly longer or shorter for the alternative structure B depending on whether the structure is calculated using B3LYP or MP2, respectively. The greatest disparity between these two structures is in the values for the angles involving the hydrogen bonds. This disparity is particularly noticeable for the ∠O₄H_{4a}O_a, which is more highly strained at 159° for structure 4A than for structure 4B at 170° at the B3LYP level of theory. At the MP2 level of theory, the values for this angle are 147 and 161° for structures 4A,B, respectively. Additional stability for alternative structure 4B comes from having two of the other hydrogen bond angles (∠O₂H_{2a}O₃ and ∠O₃H_{3a}O₄) being close to 180° compared to only one straight H bond for structure 4A. Therefore, the apparent advantage to closing the homodromic ring on the nitric acid oxygen farther away from H* is that the H-bond angles are less strained.

In agreement with McCurdy et al.,¹⁷ the first stable ion pair can be formed with four waters and nitric acid (Figure 5). The ion-pair structure for the four-water hydrate of nitric acid essentially has C_{3v} symmetry giving the H₃O⁺–NO₃⁻ pair three equivalent sets of two hydrogen-bond types. Because all three hydrogens on the hydronium ion are equivalent, they are labeled H*_{a–c} and the oxygen of the hydronium ion is labeled O_h. In this structure the H₃O⁺ sits 3.320 Å above the NO₃⁻ with the hydrogen atoms staggered relative to the oxygens of the nitrate as illustrated in Figure 5A (note that the angle is slightly canted to reveal a hint of the nitrogen atom underneath the oxygen atom of the hydronium ion). Looking at this structure, the H₃O⁺ is equally H-bonded to three other waters comprising a larger Eigen-ion⁵³ (H₅O₄⁺) moiety. The three waters form a layer between the hydronium and nitrate ions, each using one of its hydrogen atoms to form a H-bond with the nitrate while another H-bond is formed between a hydrogen of the H₃O⁺ and the water oxygen (Figure 5B). Distances for upper and lower H-bonds based on B3LYP/6-311++G(2d,p) are 1.530 and 1.746 Å, respectively. The MP2 version of these calculations gave a slightly shorter upper H-bond (1.522 Å) and longer lower H-bond (1.756 Å). Both methods gave the distance between a nitrate oxygen and a water oxygen as 2.681 Å, but the distance from the hydronium oxygen to a water oxygen was 2.555 Å compared to 2.546 Å for B3LYP and MP2 levels of theory, respectively. The upper H-bonds between a hydronium H and a water O is quite straight with an ∠O_hH*O_x (*x* = 1–3) of 172° relative to the lower H bonds between a water H and a nitrate O that have an ∠O_xH_{ya}O_y (*y* = a–c) ranging from 156 to 164° for B3LYP/6-311++G(2d,p) and MP2/6-311++G(2d,p), respectively. Other structural parameters are given in Table 8S.

On the basis of the MP2/aug-cc-pVDZ calculations, McCurdy et al.¹⁷ assigned the cyclic structure in Figure 4A as the global minimum with the ion pair (Figure 5) as a local minimum lying 0.4 kcal/mol above the cyclic structure. Our results using B3LYP/6-311++G(2d,p) and MP2/6-311++G(2d,p) confirm the order of the energies for these two structures with a difference in energy of 2.4 and 1.5 kcal/mol, respectively. The single-point MP2 energies calculated for the B3LYP/6-311++G-

(2d,p) geometries of the two structures only differ by 1 kcal/mol. However, our calculations also show that the alternative cyclic structure in Figure 4B has the lowest GS energy of all three structures, being 0.93, 0.76, or 0.27 kcal/mol below the configuration previously identified by McCurdy et al.¹⁷ as the global minimum using B3LYP/6-311++G(2d,p), spMP2 B3LYP/6-311++G(2d,p), or MP2/6-311++G(2d,p) calculations, respectively. The binding energies for these complexes are listed in Table 1. The uncorrected (D_e^{uncor}) and ZPC binding energies (D_e^{ZPC} given in parentheses) reported by McCurdy et al.¹⁷ for the cyclic and ion pair configurations were -40.5 (-31.4) and -40.1 (-29.9) kcal/mol, respectively. These values are slightly higher than the values obtained using B3LYP/6-311++G(2d,p) shown in Table 1. The binding energies for the alternative energy structure 4B are slightly higher than those of either the cyclic structure 4A or the ion-pair configuration. However, if the BSSE correction is factored in, then the binding energy of the alternative cyclic geometry 4B and the ion pair have the same binding energy of -24.3 kcal/mol. Obviously, the BSSE value is underestimated for the ion pair because it is $\sim 1/2$ of the calculated BSSE for the cyclic $\text{HNO}_3 \cdots 4\text{H}_2\text{O}$ complexes (Tables 6S–8S). This problem may be related to the symmetrical nature of the ion-pair geometry. Salvador et al.⁵⁹ have noted that, for ion/molecule interactions involving protonated species, it is potentially preferable to treat the protons involved in the H bonds as separate fragments when computing the counterpoise correction to obtain both correct structures and interaction energies. Salvador et al.⁵⁹ note that increasing the fragment types is especially important for symmetrical systems and also works well for unsymmetrical systems. This phenomenon associated with the counterpoise correction may also depend on the theory level used because the MP2 calculations did not seem to suffer from this apparent problem for the prediction of the BSSE for the ion pair. For the MP2/6-311++G(2d,p) calculations, the dissociation energy values (D_0) are -16.3 , -24.1 , and -24.9 kcal/mol for the ion-pair, cyclic, and alternative cyclic structures, respectively. The order of binding energies using MP2 is as expected given the relative overall energies for the structures.

While the results described above are instructive for isolated clusters that may be relevant to atmospheric chemistry, for solvated systems it is useful to look at the TS's because the waters are always in flux. The TS structures for the cyclic four-water systems and the ion pair are given in Figures 6 and 7, respectively. The TS for the cyclic structure 4A in Figure 6A is very similar to the TS structures for the two- and three-water systems with the sequential shuffling of hydrogen atoms around the ring with approximately equal displacements (see Table 6S). The TS for the alternative cyclic structure 4B in Figure 6B is somewhat different in that the fourth water molecule is essentially pushed over to the side so that the third water molecule can make a H bond with O_a as well as with the fourth water molecule (see Table 7S). Therefore, the structure of the GS allows all three of the nitrate oxygens to participate in H bonding in the TS; however, the displacement vectors show that of the six H bonds in the TS structure, only two hydrogens (H_{2a} and H_{3b}) experience significant displacements. The ion-pair structure in Figure 7 has lost the symmetry of the GS (Figure 5) because only one set of H bonds (involving H_c^* and H_{3a}) is involved with the proton shuffle (see Table 9S). Therefore, the TS for the alternative cyclic structure 4B can be thought of as a hybrid between the approximately equal H displacements around the ring for cyclic structure 4A and the two H displacements for the ion pair. The values for the

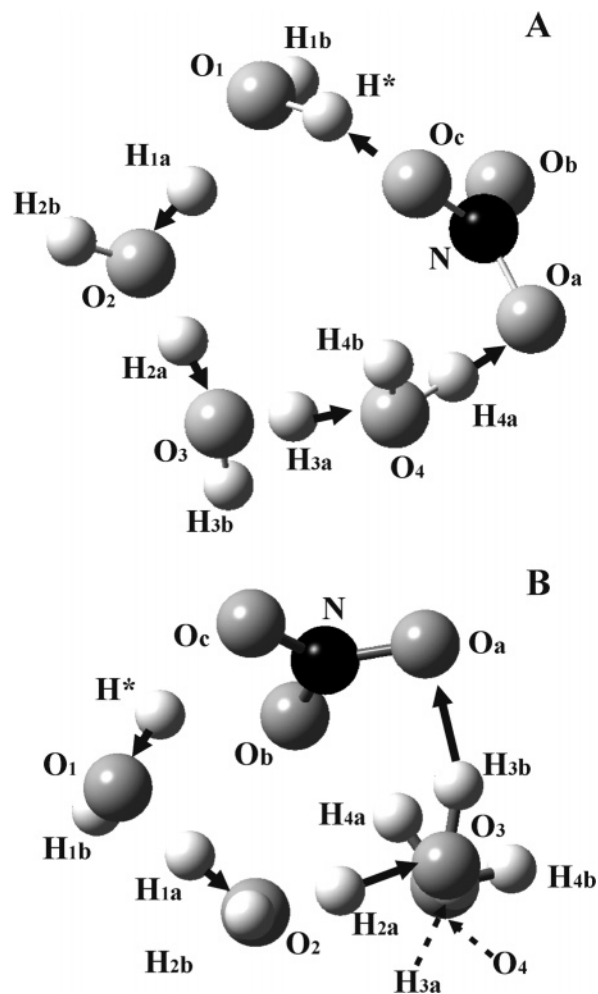


Figure 6. TS structures for two different cyclic geometries for the $\text{HNO}_3 \cdots 4\text{H}_2\text{O}$ cluster: (A) cyclic structure 4A and (B) alternative cyclic structure 4B. Solid arrows indicate displacement vectors. Color scheme is nitrogen = black, oxygen = gray, and hydrogen = white.

uncorrected TS barriers using B3LYP/6-311++G(2d,p) for the cyclic 4A, alternative cyclic 4B, and ion-pair configurations are 9.3, 8.2, and 2.8 kcal/mol, respectively. With zero-point corrections, these values drop to 7.2, 7.0, and 0.5 kcal/mol, respectively. The TS barrier for the ion pair is significantly below the other structures, which makes it closer to that for transfer of protons in water.⁴⁵ On the basis of these results, it appears that if four waters are around the nitric acid in positions similar to that for the ion pair, then there is almost no barrier to prevent the H^* of the nitric acid from moving off to form H_3O^+ , leaving NO_3^- behind.

$\text{HNO}_3 + n\text{H}_2\text{O}$ ($n > 4$) Systems. Large clusters of water with nitric acid were also investigated for up to 32 H_2O molecules. As the number of water molecules increases, the number of alternative starting geometries escalates exponentially. These calculations are also quite taxing on computer resources, especially for the higher MP2 level of theory. Several minima were determined for $n = 5-8, 14, 16,$ and 32 . The structures are not shown because they are too complicated to be rendered into meaningful two-dimensional images; however, there are some noteworthy observations. In all cases, the minima structures form an ion-pair scenario that only differs in how many waters separate H_3O^+ and NO_3^- . For lower values of n , the ion-pair motif of the $\text{HNO}_3 \cdots 4\text{H}_2\text{O}$ complex dominates as expected. As the number of waters increase, one or two more layers of H_2O molecules separate the H_3O^+ moiety from the

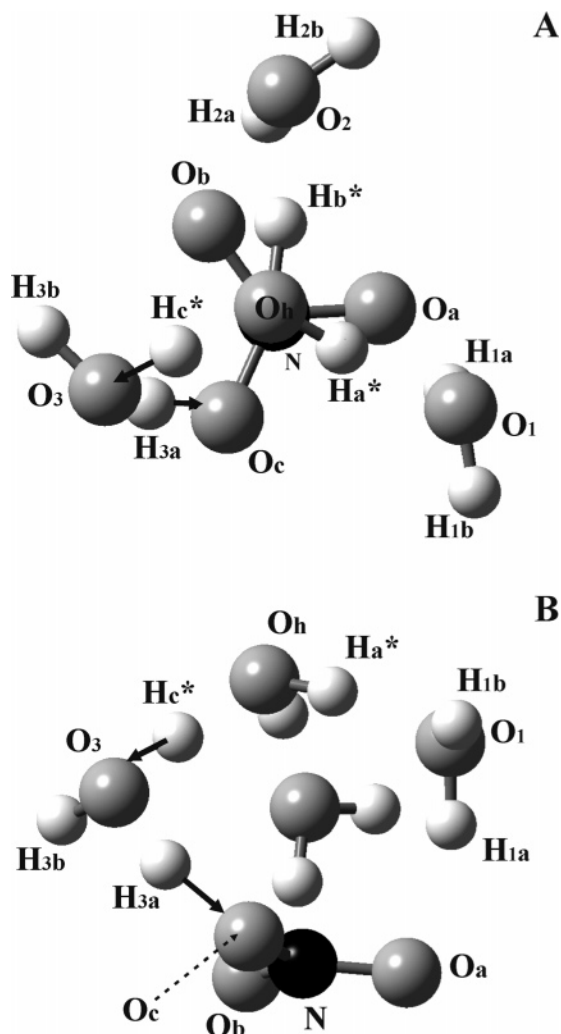


Figure 7. TS structure for $\text{HNO}_3 \cdots 4\text{H}_2\text{O}$ cluster geometry of the NO_3^- and H_3O^+ ion pair. (A) Side view of the geometry with labels for the second H_2O in the background left out for clarity. (B) Top-down view with the H_3O^+ over the NO_3^- . Solid arrows indicate displacement vectors. Color scheme is nitrogen = black, oxygen = gray, and hydrogen = white.

NO_3^- . It appears to take ~ 32 waters to fully solvate both the NO_3^- and H_3O^+ (waters all around each ion) in the gas-phase calculations. This is not surprising given that hydration of H_3O^+ alone has been found to be more stable when $n > 30$ water molecules.⁶⁰ However, even with 32 waters, the H_3O^+ often migrates to the edge of the cluster with two to three water layers between it and the NO_3^- . As with the other hydrated nitric acid configurations, the potential energy surface is very shallow making identification of a global minimum essentially meaningless. The solvation structure, H_3O^+ hydrogen bonded to three other waters to form the Eigen-ion moiety, migrates through the solvent by proton conduction as the atoms that compose the motif change as the H bonds shuffle between the water molecules. While most of the minima in complexes where $n > 7$ have a solvated proton with the H_3O_4^+ motif, in solution the solvation of the proton is in flux and other proton-water structures, such as the H_5O_2^+ , are formed.⁵¹ For these large solvated systems, it would be more useful to acquire statistics related to the separation of H_3O^+ and NO_3^- using molecular dynamics simulations.

Conclusions

Comparison of DFT B3LYP and ab initio MP2 methods using the basis set 6-311++G(2d,p) to study the complexes of

$\text{HNO}_3 \cdots n\text{H}_2\text{O}$ ($n = 1-4$) reveals that the overall results are quite similar, especially for the predicted geometries. However, there are some discrepancies in the energy calculations. These variations are probably due to the rather shallow potential energy surfaces for the interaction of HNO_3 with H_2O . The addition of a water to the cluster increases the binding energy by ~ 10 kcal/mol. For the cyclic structures, the TS barrier decreases by 1–2 kcal/mol with each additional water. According to the computations, at least four water molecules are required to ionize nitric acid to produce the $\text{H}_3\text{O}^+ - \text{NO}_3^-$ ion pair. The TS for the ion pair dropped dramatically to 0.5 kcal/mol. This ion-pair motif is maintained in clusters where $n > 4$. This implies that, in the less than fully solvated nuclear waste with nitric acid, at least four waters would need to be present around nitric acid to form the $\text{H}_3\text{O}^+ - \text{NO}_3^-$ ion pair. Future work needs to focus on the effect that other ions present in the nuclear waste have on the hydration/solvation of the nitric acid, and vice versa, because they may very well influence the polarizability of the hydrogen bonds.⁶¹

Acknowledgment. The authors gratefully acknowledge funding support of the Environmental Systems Research program, United States Department of Energy, under Contract No. DE-AC07-99ID13727 BBWI.

Supporting Information Available: Figure 1S gives structures of the monomer units HNO_3 , NO_3^- , H_2O , and H_3O^+ with the detailed parameters in Table 1S. The detailed structural and energy parameters for GS and TS geometries for various $\text{HNO}_3 \cdots n\text{H}_2\text{O}$ ($n = 1-4$) configurations are given in Tables 2S–9S. This material is available free of charge via the Internet at <http://pubs.acs.org>.

References and Notes

- (1) Canagaratna, M.; Phillips, J. A.; Ott, M. E.; Leopold, K. R. *J. Phys. Chem. A* **1998**, *102*, 1489–1497.
- (2) Gard, E. E.; Kleeman, M. J.; Gross, D. S.; Hughes, L. S.; Allen, J. O.; Morrical, B. D.; Fergenson, D. P.; Dienes, T.; Galli, M. E.; Johnson, R. J.; Cass, G. R.; Prather, K. A. *Science* **1998**, *279*, 1184–1187.
- (3) Bickmore, B. R.; Nagy, K. L.; Young, J. S.; Drexler, J. W. *Environ. Sci. Technol.* **2001**, *35*, 4481–4486.
- (4) Dietz, M. L.; Horwitz, E. P.; Sajdak, L. R.; Chiarizia, R. *Talanta* **2001**, *54*, 1173–1184.
- (5) Chambliss, C. K.; Haverlock, T. J.; Bonnesen, P. V.; Engle, N. L.; Moyer, B. A. *Environ. Sci. Technol.* **2002**, *36*, 1861–1867.
- (6) Hobbs, D. T. *Sep. Purif. Technol.* **1999**, *15*, 239–253.
- (7) Barnes, C. M.; Janikowski, S. K.; Millet, C. B. *Feed composition for the sodium-bearing waste treatment process*; INEEL/EXT-2000-01378 Rev. 3; Idaho National Engineering and Environmental Laboratory: Idaho Falls, ID, 2003.
- (8) Ritzhaupt, G.; Devlin, J. P. *J. Phys. Chem.* **1977**, *81*, 521–525.
- (9) Ritzhaupt, G.; Devlin, J. P. *J. Phys. Chem.* **1991**, *95*, 90–95.
- (10) Naganawa, H.; Tachimori, S. *Bull. Chem. Soc. Jpn.* **1994**, *67*, 2690–2699.
- (11) Koller, J.; Hadži, D. *J. Mol. Struct.* **1991**, *247*, 225–236.
- (12) Potier, A.; Poteir, J.; Herzog-Cance, M. H.; Pham Thi, M. In *Raman Spectroscopy*; Lascombe, J., Huang, P. V., Eds.; Wiley: Chichester, U.K., 1982.
- (13) Herzog-Cance, M. H.; Potier, J.; Potier, A.; Dhameincourt, P.; Sombret, B.; Wallart, F. *J. Raman Spectrosc.* **1978**, *7*, 303–310.
- (14) Tao, F. M.; Higgins, K.; Klemperer, W.; Nelson, D. D. *Geophys. Res. Lett.* **1996**, *23*, 1797–1800.
- (15) Tóth, G. *J. Phys. Chem. A* **1997**, *101*, 8871–8876.
- (16) Staikova, M.; Donaldson, D. J. *J. Phys. Chem. Chem. Phys.* **2001**, *3*, 1999–2006.
- (17) McCurdy, P. R.; Hess, W. P.; Xantheas, S. S. *J. Phys. Chem. A* **2002**, *106*, 7628–7635.
- (18) Escibano, R.; Couceiro, M.; Gomez, P. C.; Carrasco, E.; Moreno, M. A.; Herrero, V. J. *J. Phys. Chem. A* **2003**, *107*, 651–661.
- (19) Frisch, M. J.; Trucks, G. W.; Schlegel, H. B.; Scuseria, G. E.; Robb, M. A.; Cheeseman, J. R.; Zakrzewski, V. G.; Montgomery, J. A., Jr.; Stratmann, R. E.; Burant, J. C.; Dapprich, S.; Millam, J. M.; Daniels, A. D.; Kudin, K. N.; Strain, M. C.; Farkas, O.; Tomasi, J.; Barone, V.; Cossi,

- M.; Cammi, R.; Mennucci, B.; Pomelli, C.; Adamo, C.; Clifford, S.; Ochterski, J.; Petersson, G. A.; Ayala, P. Y.; Cui, Q.; Morokuma, K.; Malick, D. K.; Rabuck, A. D.; Raghavachari, K.; Foresman, J. B.; Cioslowski, J.; Ortiz, J. V.; Stefanov, B. B.; Liu, G.; Liashenko, A.; Piskorz, P.; Komaromi, I.; Gomperts, R.; Martin, R. L.; Fox, D. J.; Keith, T.; Al-Laham, M. A.; Peng, C. Y.; Nanayakkara, A.; Gonzalez, C.; Challacombe, M.; Gill, P. M. W.; Johnson, B. G.; Chen, W.; Wong, M. W.; Andres, J. L.; Head-Gordon, M.; Replogle, E. S.; Pople, J. A. *Gaussian 98*, revision A.4 ed.; Gaussian, Inc.: Pittsburgh, PA, 1998.
- (20) Frisch, M. J.; Trucks, G. W.; Schlegel, H. B.; Scuseria, G. E.; Robb, M. A.; Cheeseman, J. R.; Montgomery, J. A., Jr.; Vreven, T.; Kudin, K. N.; Burant, J. C.; Millam, J. M.; Iyengar, S. S.; Tomasi, J.; Barone, V.; Mennucci, B.; Cossi, M.; Scalmani, G.; Rega, N.; Petersson, G. A.; Nakatsuji, H.; Hada, M.; Ehara, M.; Toyota, K.; Fukuda, R.; Hasegawa, J.; Ishida, M.; Nakajima, T.; Honda, Y.; Kitao, O.; Nakai, H.; Klene, M.; Li, X.; Knox, J. E.; Hratchian, H. P.; Cross, J. B.; Adamo, C.; Jaramillo, J.; Gomperts, R.; Stratmann, R. E.; Yazyev, O.; Austin, A. J.; Cammi, R.; Pomelli, C.; Ochterski, J. W.; Ayala, P. Y.; Morokuma, K.; Voth, G. A.; Salvador, P.; Dannenberg, J. J.; Zakrzewski, V. G.; Dapprich, S.; Daniels, A. D.; Strain, M. C.; Farkas, O.; Malick, D. K.; Rabuck, A. D.; Raghavachari, K.; Foresman, J. B.; Ortiz, J. V.; Cui, Q.; Baboul, A. G.; Clifford, S.; Cioslowski, J.; Stefanov, B. B.; Liu, G.; Liashenko, A.; Piskorz, P.; Komaromi, I.; Martin, R. L.; Fox, D. J.; Keith, T.; Al-Laham, M. A.; Peng, C. Y.; Nanayakkara, A.; Challacombe, M.; Gill, P. M. W.; Johnson, B.; Chen, W.; Wong, M. W.; Gonzalez, C.; Pople, J. A. *Gaussian 03*, revision B.03; Gaussian, Inc.: Pittsburgh, PA, 2003.
- (21) Becke, A. D. *J. Chem. Phys.* **1993**, *98*, 5648–5652.
- (22) Lee, C. T.; Yang, W. T.; Parr, R. G. *Phys. Rev. B* **1988**, *37*, 785–789.
- (23) Ditchfield, R.; Hehre, W. J.; Pople, J. A. *J. Chem. Phys.* **1971**, *54*, 724–728.
- (24) Hehre, W. J.; Ditchfield, R.; Pople, J. A. *J. Chem. Phys.* **1972**, *56*, 2257–2261.
- (25) Hariharan, P. C.; Pople, J. A. *Mol. Phys.* **1974**, *27*, 209–214.
- (26) Hariharan, P. C.; Pople, J. A. *Theor. Chim. Acta* **1973**, *28*, 213–222.
- (27) Gordon, M. S. *Chem. Phys. Lett.* **1980**, *76*, 163–168.
- (28) Binning, R. C.; Curtiss, L. A. *J. Comput. Chem.* **1990**, *11*, 1206–1216.
- (29) Krishnan, R.; Frisch, M. J.; Pople, J. A. *J. Chem. Phys.* **1980**, *72*, 4244–4245.
- (30) Möller, C.; Plesset, M. S. *Phys. Rev.* **1934**, *46*, 618–622.
- (31) Peng, C. Y.; Schlegel, H. B. *Isr. J. Chem.* **1993**, *33*, 449–454.
- (32) Peng, C. Y.; Ayala, P. Y.; Schlegel, H. B.; Frisch, M. J. *J. Comput. Chem.* **1996**, *17*, 49–56.
- (33) Tao, F. M.; Pan, Y. K. *J. Phys. Chem.* **1991**, *95*, 3582–3588.
- (34) Peterson, K. A.; Dunning, T. H. *J. Chem. Phys.* **1995**, *102*, 2032–2041.
- (35) van Mourik, T.; Dunning, T. H. *J. Chem. Phys.* **1997**, *107*, 2451–2462.
- (36) Woon, D. E.; Dunning, T. H.; Peterson, K. A. *J. Chem. Phys.* **1996**, *104*, 5883–5891.
- (37) Boys, S. F.; Bernardi, F. *Mol. Phys.* **1970**, *19*, 553.
- (38) Donaldson, D. J. *J. Phys. Chem. A* **1999**, *103*, 62–70.
- (39) Frisch, M. J.; Delbene, J. E.; Binkley, J. S.; Schaefer, H. F. *J. Chem. Phys.* **1986**, *84*, 2279–2289.
- (40) van Duijneveldt, F. B.; van Duijneveldt–van de Rijdt, J. G. C. M.; van Lenthe, J. H. *Chem. Rev.* **1994**, *94*, 1873–1885.
- (41) Gutowski, M.; van Duijneveldt–van de Rijdt, J. G. C. M.; van lenthe, J. H.; van Duijneveldt, F. B. *J. Chem. Phys.* **1993**, *98*, 4728–4738.
- (42) Tzeli, D.; Mavridis, A.; Xantheas, S. S. *Chem. Phys. Lett.* **2001**, *340*, 538–546.
- (43) Schwenke, D. W.; Truhlar, D. G. *J. Chem. Phys.* **1985**, *82*, 2418–2426.
- (44) Rabuck, A. D.; Scuseria, G. E. *Theor. Chem. Acc.* **2000**, *104*, 439–444.
- (45) Agmon, N. *Chem. Phys. Lett.* **1995**, *244*, 456–462.
- (46) Nienhuys, H.-K. Ph.D. Dissertation, Technische Universiteit Eindhoven, 2002.
- (47) de Gröthuss, C. J. T. *Ann. Chim.* **1806**, *58*, 54–74.
- (48) Danneel, H. Z. *Elektrochem.* **1905**, *11*, 248–252.
- (49) Hückel, E. Z. *Elektrochem.* **1928**, *34*, 546–562.
- (50) Tulub, A. A. *J. Chem. Phys.* **2004**, *120*, 1217–1222.
- (51) Tuckerman, M.; Laasonen, K.; Sprik, M.; Parrinello, M. *J. Phys. Chem.* **1995**, *99*, 5749–5752.
- (52) Bernal, J. D.; Fowler, R. H. *J. Chem. Phys.* **1933**, *1*, 515–548.
- (53) Eigen, M.; Wicke, E. *J. Phys. Chem.* **1954**, *58*, 702–714.
- (54) Paddison, S. J.; Pratt, L. R.; Zawodzinski, T.; Reagor, D. W. *Fluid Phase Equilib.* **1998**, *151*, 235–243.
- (55) Arstila, H.; Laasonen, K.; Laaksonen, A. *J. Chem. Phys.* **1998**, *108*, 1031–1039.
- (56) Schiöberg, D.; Zundel, G. Z. *Phys. Chem. (Frankfurt)* **1976**, *102*, 169–174.
- (57) Tuckerman, M. E.; Marx, D.; Klein, M. L.; Parrinello, M. *Science* **1997**, *275*, 817–820.
- (58) Eikerling, M.; Paddison, S. J.; Zawodzinski, T. A. *J. New Mater. Electrochem. Syst.* **2002**, *5*, 15–23.
- (59) Salvador, P.; Duran, M.; Dannenberg, J. J. *J. Phys. Chem. A* **2002**, *106*, 6883–6889.
- (60) Brodskaya, E.; Lyubartsev, A. P.; Laaksonen, A. *J. Phys. Chem. B* **2002**, *106*, 6479–6487.
- (61) Schiöberg, D.; Zundel, G. *Can. J. Chem.* **1976**, *54*, 2193–2200.